



CHARACTERIZATION OF ASPHALT USING NEURAL NETWORK AND IMAGE ANALYSIS TECHNIQUE

^a Samreen Sajjad*, ^b Naveed Ahmad, ^c Afaq Ahmad

a: Transportation Engineering department, Uet Taxila, samreensjjd@gmail.com

Abstract- Artificial neural networks (ANN) and image processing (IP) are significant computer science methodologies. These methods are employed to forecast the properties of asphalt binder. To evaluate the asphalt binder's parameters, i.e., homogeneity and volumetrics, by performing a job mix formula. Several tests were conducted in the laboratory with different types of aggregate, i.e., Margallah, Sargodha, Sakhi Sarwar, and Rohi with bitumen material. The IP and ANN approaches were used in this investigation are appropriately mixed and are used to forecast the volumetrics of asphalt, i.e., air voids (Va), percent voids filled with asphalt (VFA), and voids in mineral aggregate (VMA). For this specimen, bitumen and aggregate were cast with 3.5, 4.0, 4.5, 5.0, and 5.5 aggregate grading. Two sets of specimens were created from them: (i) to determine air voids (Va), percent voids filled with asphalt (VFA), and voids in mineral aggregate (VMA); and (ii) to create an image database. An image of the top view is needed for image capturing which is taken by a smart phone. Preprocessing is performed on the obtained data (converted to grayscale, cropped, and resized to 256 256 pixels), and using the ANN method, the statistical features are collected to evaluate the VA, VMA, and VFA. The actual values of the job mix formula were differentiated from the relative values evaluated by the given methods, i.e., IP and ANN. The data set has a massive effect on the reliability of the conclusions.

Keywords- Artificial neural network, Image processing, Job mix formula, Volumetrics.

1 Introduction

In civil engineering, HMA asphalt binder is the most important material for paving highways. As laboratory testing is used to forecast the features of HMA asphalt binder for its attainment of results, which is a very laborious, time-consuming and expensive method. To overcome this problem is the use of image processing.[1] The dataset obtained from the image computation are then correlated with laboratory computations. The results obtained by image computations were quite close to laboratory computations. Both IP and ANN are used as tools to calculate the information obtained through an image. Digital cameras are used for inspection and monitoring [2].

The use of image processing helps us to investigate the homogeneity of HMA asphalt binder. So, determining the homogeneity of HMA asphalt binder through images requires a smart phone and a computer. To achieve this, IP and ANN algorithms were generated to evaluate the attributes of asphalt binder. There are two machine learning techniques. These are ANN and ANFIS, which have a great ability to forecast. The Human brain process is similar to ANN and ANFIS as it follows the relationship between neurons[2].

The properties of HMA Asphalt binder depends on the homogeneity of the HMA asphalt concrete. There are a factors which play a key role in distribution of aggregate and asphalt binder i.e. Gradation of aggregate, temperature, and compaction of the asphalt mixture[3]. In the HMA pavement homogeneity Asphalt is due to the quality of distribution of aggregate. The performance of the pavement is stimulated by the homogeneity of HMA asphalt concrete. The pavement surface is used to estimate the homogeneity of HMA asphalt concrete. This homogeneity is not estimated from inside the pavement. The macroscopic indicators of HMA asphalt concrete are porosity; density and texture depth. These macroscopic indices reflect the homogeneity of the asphalt mixture [4].

The volumetric parameters of HMA asphalt concrete are air voids, percent voids filled with asphalt and voids filled with mineral aggregate. These parameters are established by numerous laboratory tests. Air voids in HMA Asphalt are directly



related to moisture damage, rusting and fatigue life. A value of 3–5% for air voids in 2006 is recommended by NCHRP 567. This value has been used until now. A range of 7-9 micro meters for workability and rutting resistance, which was suggested by NCHRP 673 in 2011, has been used until now. A criterion for voids in mineral aggregate, which was proposed by NCHRP in 2006, is 1.5 % to 2.0 % above the minimum value. To predict whether the designed mix is workable or not, this can be done with the aid of volumetric parameter[5].

Li cong and jiachen shi[3] the images of paved asphalt mixtures were used to estimate the segregation of compacted asphalt mixture. An image processing method was used to classify the images of the paved asphalt mixture. Those images were captured during construction. There are 224 samples of HMA asphalt mixture. Images were captured from these samples for segregation detection. In this study, GLCM was used to estimate features like contrast, correlation, etc. A Naïve Bayesian classifier is used to classify the segregation of asphalt mixture images. The accuracy rate of naïve Bayesian classifier is 80% when compared to manually labelled results. The distribution of aggregates after paving can be used to characterise the distribution of aggregates in the finished pavement.

Cristine yohana ribas and Liseanepa dihlathives[6] There are three methods adopted for compaction ,i.e., impact, kneading and vibration. These three methods are then correlated with the compaction carried out in the field. It was studied whether compaction methods could be used for analysis, which is done with software. The Marshall and gyratory compactors was the most representative of the field compacted. The compactor was best approximated in the field. Results for the samples' macro-structural parameters that were acquired in the lab and those that were collected in the field were compared. There is a greater flexibility shown in results by Marshall Compactor. The results show that the super pave gyratory compactor is the most accurate method of compaction with a gyration angle of 1.25 under Brazilian conditions.

Muhammad A, Abed, zahir noori M.taki[7] In flexible pavement, tensile related cracking is a major defect. An artificial neural network (ANN) is designed to interpret the effects of nature. In this paper by the construction of the ANN model is used to predict the stiffness of asphalt. A good correlation was found between actual and estimated values. It has a coefficient of determination of 88.6%. The stiffness model's training relative error was 0.093. The discrepancy between observed and anticipated outputs is measured by this number. The relative errors for the models, nevertheless, show that there isn't much of a gap between actual values and predictions.

Vidhi vyas and ajit partap singh [8] For pavement rehabilitation and maintenance, models are developed by using the mechanisms of artificial intelligence. ANN for asphalt pavement structural condition models is developed. There are three parameters used in that network used as input data. These parameters are structural, functional, and environmental. The data is collected in the field. The accuracy of the correlations discovered in this research is predicted to raise greater perception of the significance of structural adequacy factors in asphalt M&R judgment. The use of neural network as it performs well in even case of limited data.

The aim of this research is to develop a protocol for the characterization of asphalt using image analysis techniques. The major objectives of the research work are (a) development of a setup for capturing images; (b) development of an algorithm for studying/analyzing homogeneity & volumetrics of different types of asphalt mixtures; (c) training of laboratory values (output) versus image processing results (input) in Matlab or Python; and (d) correlation of experimental and image processing results. The fundamental goal of this research work is create a model for forensic analysis of asphalt concrete. In this way, IP and ANN are used to estimate the features of HMA asphalt concrete through images. The purpose of this research work is to correlate the laboratory values (VA, VFA, and VMA) with the software values (results of images which are mean, mode, median, entropy, skewness, and third moment) and to create a model for this purpose.

In the present work, a job mix formula (ASTM D1559) which is based on IP, ANN, and ANFIS, is used to predict the properties of HMA asphalt concrete. With the use of aggregate gradation, 82 samples of varying VA, VMA, and VFA are prepared. With the use of each aggregate gradation, similar asphalt concrete samples are prepared. In a conventional test, one of the asphalt concrete samples was utilized. The second sample was used to evaluate features like mean mode etc, from the obtained HMA asphalt mixture images. To predict the properties of HMA asphalt concrete, the images were used to test and train the network.

2 Processing of Image and ANN

Processing of images is done to collect fruitful information by the using computer algorithms. Various programs, such as Matlab and Python programming[9], have been effectively utilised to interpret photographs. Digitalization is a technique in which photographs are converted into digit form by technique of image processing. A pixel from the digitally created image is represented by each element of the matrix. The fundamental logical building block of an image, a pixel, indicates



the brightness of a gray scale image's unit area. Convergence with ANNs can be utilised to solve issues by using matrices produced through image processing[10]. An algorithm based on an artificial neural network uses concepts from the human brain to tackle difficult and time-consuming tasks. The first layer of an ANN is the input layer, the second is the hidden layer, and the third is the output layer. These layers are shown in Figure 1.

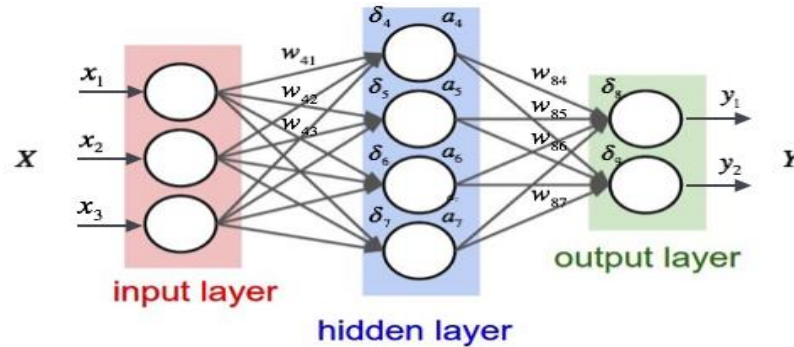


Figure 1: Connection of weight and bias to an input[2]

3 Sample Productions and Testing

It begins with material mixing and sample preparation, then moves on to image acquisition, and finally, specimen training.

3.1 Sample Preparation.

In this section, we prepared 82 samples with a Diameter 102 mm and height of 64mm as shown in Figure2.1. Only hot mixtures employing penetration grades of asphalt cement and incorporating aggregates with a maximum size of 25 mm are eligible for JMF. The key goal is to come up with an affordable and practical mix that includes the right combination of materials and the right amount of asphalt. Under traffic loading, HMA should not rut or deform (shove). Achieving fatigue life, temperature conditions cracking resistance, durability, moisture damage resistance, skid resistance, and workability is JMF's top priority. The two main ingredients of HMA are aggregate and asphalt binder. The process of deciding which aggregate to use, which asphalt binder to utilise, and what the ideal ratio of these two components should be is known as HMA mix design.

Asphalt Concrete Wearing Course Requirements

Mix Designation		Class A	Class B
Compacted Thickness		50-80 mm	35-60 mm
Combined Aggregate Grading Requirements			
Sieve Designation		Percent Passing by Weight	
Mm	Inch		
25	1	100	-
19	3/4	90-100	100
12.5	1/2	-	75-90
9.5	3/8	56-70	60-80
4.75	No. 4	35-50	40-60
2.38	No. 8	23-35	20-40
1.18	No. 16	5-12	5-15
0.075	No. 200	2-8	3-8
Asphalt Content by weight percent of total mix		3.5 (Min.)	3.5 (Min.)



Table 1: Asphalt concrete wearing course requirement Figure 2: Particle size distribution of aggregate

The aggregate is graded to measure its workability, permeability, fatigue resistance, friction resistance, stiffness, stability, durability, and resistance to moisture damage. In the JMF, the aggregate gradation is a crucial component. The prepared



aggregate is sent through a sequence of progressively smaller sieves that are stacked on top of one another. The aggregate is shaken, and as it goes through each sieve, its nominal size is determined. Sieve analysis is frequently employed to assess gradation. A sample of dry aggregate with known weight is separated using a series of sieves with progressively smaller apertures in a sieve analysis.

Size	Percentage Passing	Percentage Retained					
mm	%	%	3.50%	4%	4.50%	5%	5.5%
			Weight Retained (gm)				
25	100	0	0	0	0	0	0
19	95	5	57.9	57.6	57.3	57	56.7
9.5	63	32	370.56	368.64	366.72	364.8	362.88
4.75	42.5	20.5	237.39	236.16	234.93	233.7	232.47
2.36	29	13.5	156.33	155.52	154.71	153.9	153.09
0.3	8.5	20.5	237.39	236.16	234.93	233.7	232.47
0.075	5	3.5	40.53	40.32	40.11	39.9	39.69
Pan	-	5	57.9	57.6	57.3	57	56.7

Table 2: Aggregate gradation

Total Weight of Sample = 1200 gms				
Maximum Aggregate Size = 19 mm				
Trial Mixes	Bitumen Content	Bitumen	Aggregate Content	Aggregates
	%	gm	%	gm
1	3.5	42	96.5	1158
2	4	48	96	1152
3	4.5	54	95.5	1146
4	5	60	95	1140
5	5.5	66	94.5	1134

Table 3 Mix design criteria

Following separation, the weight of the particles retained on each sieve is determined and the weight of the entire sample is compared. The particle size distribution defined as a percent retained by weight on each filter size is shown in Table 1, Figure 2, Table 2, and Table 3. This approach uses numerous trial aggregate-asphalt binder mixes, each with a different asphalt binder content, to perform this experiment (roughly 5 blends with 3 sample each, for a total of 15 specimens). The best asphalt binder content can then be chosen after carefully examining the performance of each sample blend. The trial blends must have a range of asphalt content above and below the ideal asphalt content in order for this concept to be successful. Therefore, determining the ideal asphalt proportion is the first step in sample preparation.



Figure 2.1: Prepared samples

Trial blend asphalt content is then calculated from this appraisal. The link between asphalt mix density and voids is crucial to JMF design. To create a mix formula, two density values are used: theoretical maximum specific gravity (TMSG) and bulk specific gravity (Gmb) (Gmm). The volumetric parameters for the JMF can be computed from the Gmm value once it has been determined using a standard process recognised by the industry. For density and void calculations, the following calculations are used: (I) Bulk Specific Gravity, Gsb. (II) Effective Specific Gravity, Gse. (III) Effective Asphalt, Pbe. V) Air Voids, Va. VI) Asphalt-filled Voids, VFA Their calculations and formulas are shown in Figure 2.2, Figure 2.3, Figure 2.4, Figure 2.5, Figure 2.6, and Figure 2.7.



$$G_{ab} = \frac{P_1 + P_2 + \dots + P_N}{\frac{P_1}{G_1} + \frac{P_2}{G_2} + \frac{P_N}{G_N}}$$

Where, G_{ab} = Bulk specific gravity for the total aggregates
 P_1, P_2, P_N = Individual percentages by mass of aggregates
 G_1, G_2, G_N = Individual (e.g. coarse, fine) bulk specific gravity of aggregates.

Figure 2.2: Formula for bulk specific gravity

$$G_{se} = \frac{P_{mm} - P_b}{\frac{P_{mm}}{G_{mm}} - \frac{P_b}{G_b}}$$

G_{se} = effective specific gravity of aggregates
 G_{mm} = maximum specific gravity of paving mixes.
 P_{mm} = percent by mass of total loose mixture=100
 P_b = asphalt content at which G_{mm} test was performed, percent by total mass of mixture.
 G_b = specific gravity of asphalt.

Figure 2.3: Effective Specific Gravity

$$P_{be} = P_b - \frac{P_{ba}}{100} \times P_s$$

P_{be} = Effective asphalt content, percent by total mass of mixture
 P_b = asphalt content, percent by total mass of mixture.
 P_{ba} = absorbed asphalt, percent by mass of aggregates

Figure 2.4: Effective Asphalt, P_{be}

$$VMA = 100 - \frac{G_{mb} \times P_s}{G_{sb}}$$

VMA = voids in the mineral aggregates, percent of bulk volume.
 G_{sb} = bulk specific gravity of total aggregates
 G_{mb} = bulk specific gravity of compacted mixture
 P_s = aggregates content, percent by total mass of mixture.

Figure 2.5: Voids in mineral Aggregates

$$V_a = 100 \times \frac{G_{mm} - G_{mb}}{G_{mm}}$$

V_a = air voids in compacted mixture, percent of total volume.
 G_{mm} = maximum specific gravity of paving mixture (as determined in previous article or as determined directly for a paving mixture by ASTM D2041/AASHTO T209)
 G_{mb} = bulk specific gravity of compacted mixture

Figure 2.6: Air Voids

$$VFA = 100 \times \frac{VMA - V_a}{VMA}$$

VFA = Voids filled with asphalt, percent of VMA
VMA = Voids in the mineral aggregates, percent of bulk volume
 V_a = air voids in compacted mixture, percent of total volume.

Figure 2.7: Voids filled with Asphalt

3.2 Image Acquisition

Images of prepared HMA Asphalt samples were captured by smart phone huawei y6p. Images were captured by a smart phone having 13 megapixels with triple camera. The images of top view were taken as HMA Asphalt samples were homogenous. In pavement homogeneity of HMA Asphalt is due to quality of distribution of aggregate and asphalt. There is no need to capture images of bottom view and side view due to homogeneity of HMA asphalt binder. So, only images of top view were taken to apply computer algorithms to obtain a matrix. The collected images had a 1600×720 pixels resolution. For example there is a Matrix representation for an image as shown in Figure 2.8.



Figure 2.8: Matrix representation of an image[11]

3.3 Job mix Formula

Furthermore, the distribution of aggregate, aggregate gradation, temperature, and compaction of the asphalt mixture all has an influence on the characteristics of asphalt binder. The Marshall Mix design method consists of six basic steps. (1) Aggregate selection (2) Asphalt binder selection (3) Sample preparation (including compaction) (4) Calculation of density and voids (5) Determining stability using the Marshall Stability and Flow Test. (6) Choosing the best asphalt binder content. The preparation Specimens of HMA asphalt concrete samples containing bitumen and aggregate were examined through density voids calculations, which are given as shown in Table 4, Table 5, Table 6, and Table 7.

Binder Contents (%)	Stability, Kgs	Flow (mm)	Unit Weight Kg/m ³	Va	VMA	VFA
3.5	718.86	7.05	2302.617	8.09296	16.15	49.8887
4	818.31	7.85	2315.46	8.52705	16.1193	47.1003
4.5	911.16	8	2294.09	9.60295	17.3261	44.5388
5	958.71	8	2323.10	9.70744	16.7191	41.9363
5.5	958.71	7.7	2317.28	7.83236	17.3651	54.896

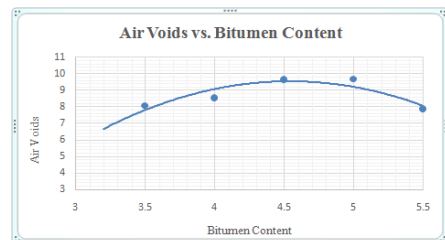


Table 4: Binder content for Sakhi Sarwar at 4.4% air voids

Binder Contents (%)	Stability, Kgs	Unit Weight Kg/m ³	Va	VMA	VFA
3.5	950.2	2367.395	5.22103	13.7911	62.142
4	1040.61	2392.84	4.694	13.361	64.7495
4.5	1114.31	2396.25	5.21577	13.644	61.7737
5	1073.37	2407.14	5.31275	13.7064	61.239
5.5	868.2	2396.04	4.98375	14.5564	65.7626

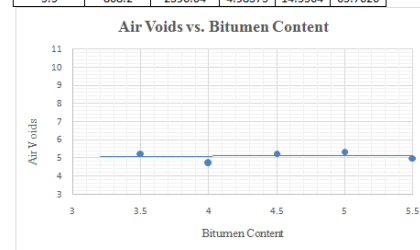
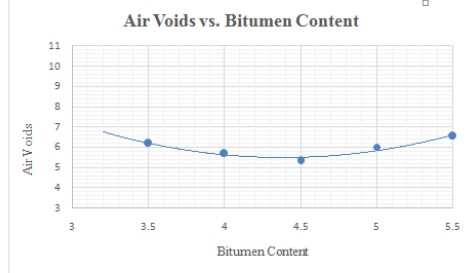


Table 5: Binder content for Sargodha at 4.0% air voids



Binder Contents (%)	Stability, Kgs	Unit Weight Kg/m ³	Va	VMA	VFA
3.5	1052.31	2308.61	6.1658	15.9266	61.2764
4	1166.97	2343.99	5.64762	15.0858	62.5693
4.5	1134.21	2368.63	5.29055	14.6399	63.8622
5	989.13	2346.32	5.97607	15.8868	62.3834
5.5	970.41	2327.36	6.5201	17.0055	61.6589



Binder Contents (%)	Stability, Kgs	Unit Weight Kg/m ³	Va	VMA	VFA
3.5	1072.59	2307.99	5.04	15.95	68.37
4	1078.83	2315.45	5.6	16.11	65.23
4.5	1127.19	2347.36	5.79	15.4	62.35
5	1004.34	2333.28	6.49	16.35	60.15
5.5	970.41	2323.88	7.14	17.12	58.3

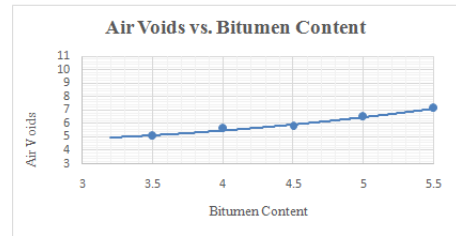


Table 6: Binder content for Rohi at 4.3% air voids Table 7: Binder content for Margallah at 3.9% air voids

4 Proposed method (IPAN)

4.1 Image processing of samples

Matlab is an image visualization tool, and images were obtained through a smart phone. These images were converted to matrices by computer algorithms. The resolution for images is 720 x 1600 with a 13 megapixel triple camera. Photographs were cut off to confine only the HMA asphalt binder part. True color photographs made up the originals (RGB images). By using Eq(1) to create a weighted sum of the R (red), G (green), and B (blue) components, the RGB images were transformed to grayscale format.

$$GS = 0.298 R + 0.589 G + 0.113 B \quad (1)$$

Where GS is the estimated grayscale component and R, G, and B stand for the red, green, and blue color components of a pixel. The grayscale photographs were then scaled to 256 256 pixels in size. The portion of the HMA asphalt sample that was cropped, scaled, grey scaled, and further processed by the computer algorithm to produce the necessary matrix is indicated by the matrix's pixel values[2]. The arithmetic mean, standard deviation, median, third moment, skewness, and entropy were estimated statistical features using Matlab code. The Levenberg-Marquardt mode was used to calculate these statistical characteristics[10]. Figures 3.1 and 3.2 contain their mathematical calculations as well as descriptions of these qualities.

Statistical features.

Feature	Expression	Description
Mean	M	Measure of average intensity
Median	Me	Middle value of pixel in an ordered column
Standard deviation	Std	Measure of average contrast
Third moment	Mo	Measure of the distribution skewness
Entropy	E	Measure of randomness in pixels
Skewness	Sk	Measure of asymmetry in matrix

Figure 3.1: Statistical features.

$$M = \frac{1}{k} \sum_{i=1}^k V_i$$

$$Me = \{(k+1) \div 2\}^{th}$$

$$Std = \sqrt{\frac{1}{k} \sum_{i=1}^k (V_i - M)^2}$$

$$Mo = \frac{1}{k} \sum_{i=1}^k (V_i - M)^3$$

$$E = - \sum_i p_i \cdot \log_2(p_i)$$

$$Sk = \frac{\frac{1}{k} \sum_{i=1}^k (V_i - M)^3}{Std^3}$$

Figure 3.2: Formulas for statistical features



Where k is the total number of data values for the variable, V displays the variables in the digitalized matrix, Me represents the median value of the pixels in the digital images, Std stands for the standard deviation, Mo for the third moment, E is entropy, p represents the normalized histogram counts, and Sk represents the skewness value. As mentioned above, there are six features, which together make up six rows and twenty-four columns (6×256).

4.2 ANN Modelling

Image processing in Matlab gives a matrix of 256 columns, and that matrix is used as an input value for image processing. Input values have features like mean, mode, standard deviation, third moment, skewness, and entropy. That input value is used for training ANN by the Levenberg-Marquardt model. The output of ANN used for its training is VA, VFA, and VMA. The values for this output are obtained by experiment in laboratory. Data from both the input and the output were normalized to lie between 0 and 1.using Eq. (2).

$$N = (V - V_{min}) / (V_{max} - V_{min}) \quad (2)$$

Where N denotes the normalized value of the variable V , while V_{min} and V_{max} are the lowest and highest values of the variable V , respectively.

4.3 Training and Testing of Data Set

After normalizing the data to a range of 0–1, then that data is used for ANN modelling by the Levenberg-Marquardt model. This program uses the ANN toolbox and we have to choose input and output variables. We will also choose the number of neurons and start training the data with a ratio of 75% training, 15% validation, and 15% testing. After the completion of the process, it will give us three plots. Tables 8 and 9 show regression plots, histogram plots, and error plots. Input is used as input data and output is used as target data.

4.4 Practical implementation of image processing

The detection of cracks in asphalt pavement using a convolution neural network [12], using random aggregate packing for computer simulation of the microstructure of asphalt concrete [1], determination of the internal asphalt structure change during the wheel tracking test [13], detection of bugholes on concrete surface[14], to evaluate segregation of compacted asphalt pavement[3] are practical image processing implementations. The practical implementation of this research work is to characterize the HMA asphalt concrete with the use of image processing.

5 Results and Discussions

In this study, amalgam of IP and ANN was used to evaluate the properties of the asphalt mixture. In the first step, IP was used to derive the matrix of images, and secondly, the matrix of this image is normalized to a range of 0-1 and thirdly. The data is trained in ANN by using the Levenberg-Marquardt model. Three sets of data are used, i.e., Training, Testing and validation of the data set. After the completion of the process, it will give us three plots. The first is the regression plot, which will give us the R value, the second is the histogram, which shows the precision of data, and the third is the error plot, which will give us the accuracy of data. The results of regression values at the overall stage obtained from the optimized (IP, ANN) model, with $R = 1$, are also depicted in Table 9. The regression value shows the accuracy of data being related to the accuracy of the model being developed. These plots are shown above in Table 8 and Table 9, Table 10, Table 11, Table 12, Table 13 and Table 14.

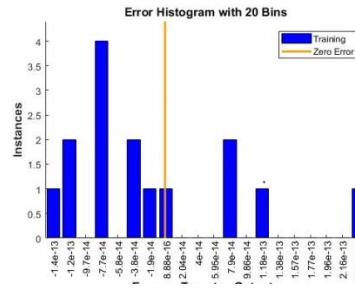


Table 8: Error histogram with 20 bins for Margallah

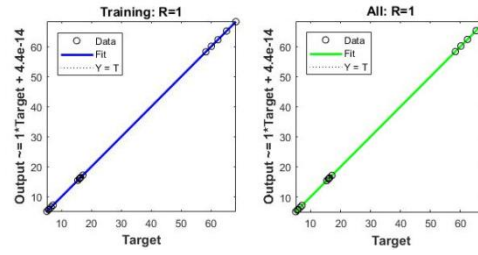


Table 9: Training and testing of data set

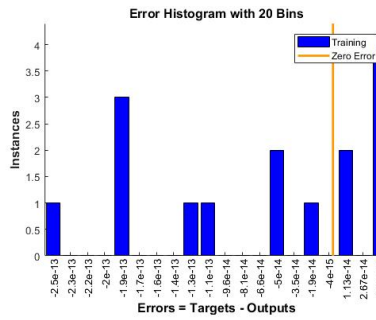


Table 10: Error histogram with 20 bins for Sargodha

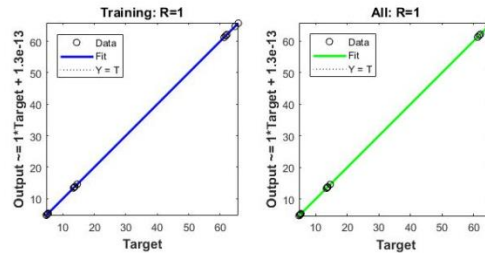


Table 11: Training and testing of data set

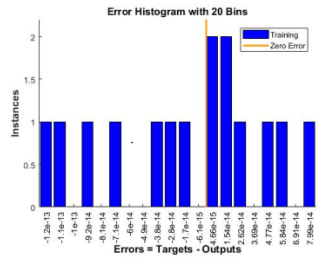


Table 11: Error histogram with 20 bins for Rohi

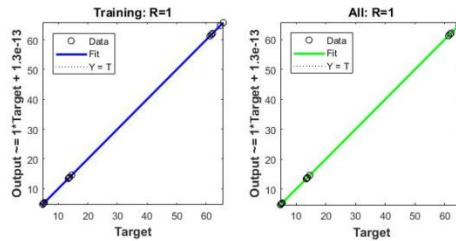


Table 12: Training and testing of data set

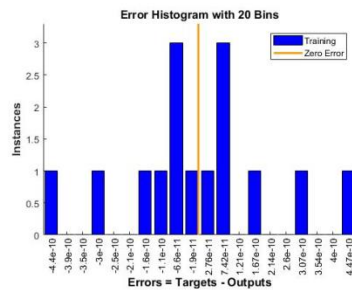


Table 13: Error histogram with 20 bins for Sakhi Sarwar

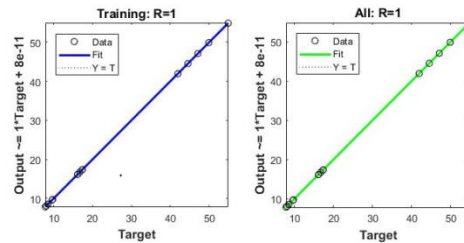


Table 14: Training and testing of data set



The error histogram is the histogram of the errors between the target values and forecasted values after a feed-forward neural network has been trained. These error values, which could be negative, demonstrate the discrepancy between the projected and goal values. Bins are how many vertical bars plotted on the graph. 20 smaller bins comprise the entire error range in this instance. In the case of Margallah, the Y-axis displays the number of instances in each bin of the dataset. For this reason, the height of the bin for the training dataset is greater than but near to 4, and it corresponds to an error of 7.7×10^{-14} in the left side of the plot. It implies that numerous samples from various datasets have an error that falls within the range given below. The error axis's zero error value is expressed by the zero error line (i.e., X-axis). The zero error point in this instance comes under the bin with a left of 8.86×10^{-14} .

The number of samples in a given bin on the dataset is shown on the Y-axis in case of Sargodha. For this purpose, in the right side of graph, there is a bin that corresponds to an error of 4.21×10^{-14} , and for the training dataset, that bin's height is greater than but not quite 4. It means that many samples from different datasets have an error lying in that following range. The zero error point in this instance is within the bin that has a right side of -4×10^{-15} .

The number of samples in a given bin on the dataset is shown on the Y-axis in case of Rohi. For this purpose, in the right side of graph, there is a bin that corresponds to an error of 4.66×10^{-15} , and that bin's height for the training dataset is greater than but not quite 2. It means that many samples from different datasets have an error lying in that following range. The zero error point in this instance is within the bin having a right side of 4.66×10^{-15} .

The number of samples in a given bin on the dataset is shown on the Y-axis in case of Sakhi Sarwar. For this purpose, in the right or left side of graph, there is bin that corresponds to an error of 1.9×10^{-11} , and For the training dataset, that bin's height is greater than but not quite 3. It means that many samples from different datasets have an error lying in that following range. The zero error point in this instance occurs beneath the bin with a centre of 4.0×10^{-12} .

However, the majority of the error comes inside the range of x-values where you can see the high bars. In the instance of Margallah, all of the error was fairly modest and falls in the range of $-1.4e-13$ to $2.5e-13$. Each bar's height represents the total number of tests, or "instances." Take note of how the orange "zero error" line divides the positive and negative ticks. You may establish the bias's direction by looking at the error's sign. On the x-axis label that specifies error as Targets-Outputs, positive error implies the outputs were less than the targets, and negative error means the targets were greater than the outputs (assuming the targets are positive values). The bulk of outputs were slightly bigger than the targets because the majority of tests were negative.

In case of Sargodha all of the error was quite low and falls in the range of $-2.5e-13$ to $4.2e-14$ but most of the error falls within the range of x-values where you see the high bars. Take note of how the orange "zero error" line divides the positive and negative ticks. You may establish the bias's direction by looking at the error's sign. On the x-axis label that specifies error as Targets-Outputs, positive error implies the outputs were less than the targets, and negative error means the targets were greater than the outputs (assuming the targets are positive values). Since most tests were negative, most outputs were a little bit greater than the targets. The same is true for Sakhi and Rohi Sarwar. Using IP, these four forms of aggregate describe the asphalt. In tables 15 and 16, a combine model for these four categories of aggregate is displayed.

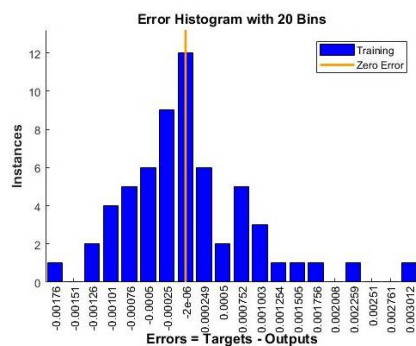


Table 15: A combine model of Data set

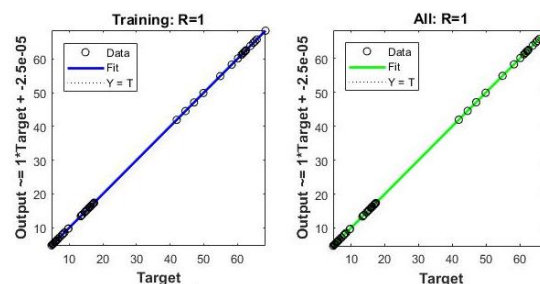


Table 16: A combine model of Regression values

Conclusions



This study has demonstrated the viability of employing an image processing technology and a smart phone to quantify the properties of HMA asphalt based on job mix formula. A number of image processing techniques are used to obtain data in the shape of a 256-column matrix. To compare the outcomes with those discovered by IP, manual lab tests were also carried out. IP characterization was demonstrated to be quicker and easier. Results from image analysis can be more accurate than those from lab tests. Average values are presented by laboratory testing, and statistical distributions for each parameter are shown by picture analysis. The data sets have a significant impact on the results' correctness. For further study, the proposed method can be used in the field. Images of pavements can be captured and then image processing procedures are adopted. This process helps to predict the properties of asphalt pavement for further study.

Acknowledgment

The structural engineering department and Engr. Dr. Afaq Ahmed in particular deserve special thanks from the authors for their assistance throughout the research project. We sincerely thank the anonymous reviewers for their thorough analysis and helpful recommendations.

References

1. Salemi, M. and H. Wang, *Image-aided random aggregate packing for computational modeling of asphalt concrete microstructure*. Construction and Building Materials, 2018. 177: p. 467-476.
2. Muhammad Imran Waris, V.P., Junaid Mir, Nida Chairman, Afaq Ahmad,, *An alternative approach for measuring the mechanical properties of hybrid concrete through image processing and machine learning*, Construction and Building Materials,, april 2022. Volume 328, 2022,: p. 16.
3. Cong, L., et al., *A method to evaluate the segregation of compacted asphalt pavement by processing the images of paved asphalt mixture*. Construction and Building Materials, 2019. 224: p. 622-629.
4. Xuelian li, Y.z., Zhanping you, *Homogeneity evaluation of hot in place recycling asphalt mixture using digital image processing technique*. journal of cleaner production, 10 june 2020.
5. Yining zhang, h.c.l., *Determination of volumetric criteria for designing hard asphalt mixture*. Construction and building material, 5 april 2021: p. 12.
6. Ribas, C.Y. and L.P. Thives, *Evaluation of effect of compaction method on the macrostructure of asphalt mixtures through digital image processing under Brazilian conditions*. Construction and Building Materials, 2019. 228: p. 116821.
7. Muhaamed a. abed, z.n.t., *Artificial neural network modeling of the modified hot mix asphalt stiffness using Bending Beam Rheometer*. materials today, 2021.
8. vidhi vyas, a.p.s., *Modeling asphalt pavement condition using artificial neural networks*. materials today proceedings, 2022.
9. masoomeh mirrashid, h.n., *Computational intelligence-based models for estimating the fundamental period of infilled reinforced concrete frames*. journal of buildind engineering, april 2022.
10. Seghier, M.E.A.B., et al., *On the modeling of the annual corrosion rate in main cables of suspension bridges using combined soft computing model and a novel nature-inspired algorithm*. Neural Comput. Appl., 2021. 33(23): p. 15969–15985.
11. gamze dogan, M.h.a., *Concrete compressive strength detection using image processing based new testConcrete compressive strength detection using image processing based new test*. 2017: p. 12.
12. Nhat-Duc, H., Q.-L. Nguyen, and V.-D. Tran, *Automatic recognition of asphalt pavement cracks using metaheuristic optimized edge detection algorithms and convolution neural network*. Automation in Construction, 2018. 94: p. 203-213.
13. Ni, J.J.F., *Investigation of the internal structure change of two-layer asphalt mixtures during the wheel tracking test based on 2D image analysis*. Construction and Building Materials, 10 june 2019.
14. Baoju Liu, T.Y.a., *Image analysis for detection of bugholes on concrete surface*. Construction and Building Materials, 15 april 2017.